Ceramics International xx (xxxx) xxxx–xxxx

Contents lists available at ScienceDirect

Ceramics International

journal homepage: www.elsevier.com/locate/ceramint

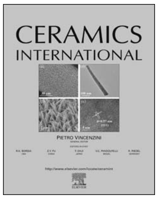

Influence of moisture absorption on the synthesis and properties of Y_2O_3–MgO nanocomposites

Junxi Xie[a,b], Xiaojian Mao[a,*], Xiaokai Li[a], Benxue Jiang[a], Long Zhang[a,*]

[a] *Key Laboratory of Materials for High Power Lasers, Shanghai Institute of Optics and Fine Mechanics, Chinese Academy of Sciences, Shanghai 201800, China*
[b] *The University of Chinese Academy of Sciences, Beijing 100049, China*

A R T I C L E I N F O

Keywords:
Y_2O_3–MgO nanocomposites
Nanopowders
Moisture absorption
Water resistance

A B S T R A C T

Y_2O_3–MgO nanocomposites are appropriate materials for hypersonic infrared windows and domes because of their low emissivity and improved mechanical properties. In this study, the synthesized Y_2O_3–MgO nanopowders are investigated to evaluate the influence of moisture absorption on the manufacturing process and properties of the resulting nanocomposites. It is shown that MgO plays a more significant role than Y_2O_3 in the moisture absorption of the composite nanopowders, and the absorbed moisture leads to a lowering IR transmittance of the final Y_2O_3–MgO nanocomposites. A higher calcination temperature improves the resistance to moisture absorption of Y_2O_3–MgO nanopowders, which is beneficial for IR transmittance of the final nanocomposites. In addition, increasing the sintering temperature to 1100 °C during spark plasma sintering (SPS) minimizes the influence of absorbed moisture on the IR transmittance of the final nanocomposites. In the water resistance test, the Y_2O_3–MgO nanocomposites demonstrate severely eroded surfaces and degraded IR transmittance after water erosion, suggesting the requirement for necessary water-proof treatments on such materials in practical applications.

1. Introduction

In recent years, there has been a growing tendency to use polycrystalline transparent ceramics as infrared windows and domes because of their favorable mechanical and optical properties [1–6]. However, the development of advanced hypersonic missiles with faster speed and higher accuracy requires infrared windows and domes with increased mechanical strength, modified thermal shock resistance and lower emissivity. Among the commonly available and durable mid-infrared materials, polycrystalline Y_2O_3 has a lower emissivity and superior high-temperature optical transmittance, but the unsatisfactory mechanical properties restrict their application in hypersonic vehicles [5]. Nano-ceramics have received considerable attention because of their improved mechanical and optical properties [7–11]. Harris [12] and Jiang [13] introduced MgO nanoparticles in the manufacture of Y_2O_3–MgO nanocomposites with a bending strength of up to 660 MPa, because the presence of one phase inhibits the grain growth of the adjacent phase. This inhibition of grain growth is beneficial for improved mechanical strength. It is predicted and approved that the nanocomposites are infrared transparent as the grain size is much smaller than the wavelength of the incident light [14]. Several synthetic methods based on esterification [15], redox reactions [16], and combustion [17] have been developed to prepare Y_2O_3–MgO nanopowders. Moreover, pressure-assisted sintering methods, such as hot pressing (HP) and spark plasma sintering (SPS), have been employed for consolidation of such nanocomposites [17,18].

However, the fabrication of Y_2O_3–MgO nanocomposites with excellent optical and mechanical properties is still a challenge when considering the rigorous requirements of practical application. A noteworthy issue, which has not been regarded so far, is that both Y_2O_3 and MgO absorb moisture when exposed to ambient atmospheres [19,20]. It could be expected that the moisture absorption of Y_2O_3–MgO nanopowders will affect the optical transmittance of the obtained nanocomposites. Besides, Y_2O_3–MgO nanocomposites might not have effective resistance against water erosion. The possible exposure to raindrops in practical application would induce further erosion, leading to unexpected mechanical disruption or optical degradation. The purpose of the present work is not only to seek an appropriate treatment of the prepared nanopowders to improve the transmittance of the resulting nanocomposites, but also to investigate the different hygroscopic behaviors of Y_2O_3 and MgO in the composite nanopowders and the influence of water erosion on the optical property of the

---

* Corresponding authors.
E-mail addresses: xmao@siom.ac.cn (X. Mao), lzhang@siom.ac.cn (L. Zhang).

http://dx.doi.org/10.1016/j.ceramint.2016.08.117
Received 13 July 2016; Received in revised form 17 August 2016; Accepted 18 August 2016
Available online xxxx

Please cite this article as: Xie, J., Ceramics International (2016), http://dx.doi.org/10.1016/j.ceramint.2016.08.117

resulting nanocomposites.

2. Experimental

Y_2O_3–MgO nanopowders were synthesized by sol–gel combustion method, as described elsewhere [21]. $Y(NO_3)_3 \cdot 6H_2O$ (99.99%, Tianjin Fine Chemicals, Tianjin, China), $Mg(NO_3)_2 \cdot 6H_2O$ (99.99%, Tianjin Fine Chemicals, Tianjin, China), citric acid monohydrate (Sinopharm Chemical Reagent Co., Ltd., AR, Shanghai, China), and ethylene glycol (Sinopharm Chemical Reagent Co., Ltd., AR, Shanghai, China) were used as raw materials. Firstly, aqueous solutions of 4 mol/L $Y(NO_3)_3 \cdot 6H_2O$ and 8 mol/L $Mg(NO_3)_2 \cdot 6H_2O$ were prepared using distilled deionized water. Next, 9.82 g citric acid monohydrate and 1.45 g ethylene glycol were dissolved in 100 mL of distilled deionized water in a 600 mL glass beaker. Subsequently, 10 mL of 4 mol/L $Y(NO_3)_3 \cdot 6H_2O$ and 10 mL of 8 mol/L $Mg(NO_3)_2 \cdot 6H_2O$, corresponding to Y_2O_3 and MgO volume ratio of (50:50), were sequentially poured into the glass beaker. After stirring for 15 min, this solution was heated at 200 °C until the porous organic foams were formed. They were then converted to brown fluffy powders by a self-sustaining combustion reaction. Eventually, these powders were placed in a muffle furnace, calcined to predetermined temperatures at a heating rate of 1 °C/min, and then held for 2 h.

The calcined nanopowders were ball-milled using 2 mm ZrO_2 balls in anhydrous alcohol for 48 h. The slurry was dried at 70 °C and sieved through a 200-mesh screen. The as-prepared nanopowders were loaded into a graphite die, and heated from 25 °C to 1000 °C at 100 °C/min under vacuum (~6 Pa). They were held at that temperature for 8 min before the power was turned off. The powders were gradually consolidated by SPS. The load was low initially, but was gradually increased to 70 MPa. The fabricated nanocomposites were annealed at 1000 °C for 15 h in air and then polished on both sides for optical characterization. Furthermore, the polished nanocomposites were immersed in distilled deionized water for 7 d to investigate water erosion resistance.

Powder X-ray diffraction (XRD, PANalytical X'Pert Pro, Netherlands) analysis was carried out for analyzing crystalline phases of the synthesized powders, and the Scherrer formula was used as a supplementary support to estimate the crystallite size. The specific surface area of the Y_2O_3–MgO nanopowders was determined using a N_2 adsorption apparatus (Quadra orb SI, America) based on the multipoint Brunauer-Emmet-Teller (BET) isotherm. The morphologies of the prepared samples were characterized by field emission-scanning electron microscopy (FE-SEM, ZEISS, Germany) and transmission electron microscopy (TEM, JEM-2100F, Japan). Fourier transform infrared (FT-IR, Nicolet 6700, Thermo Nicolet, USA) spectroscopy in the transmittance mode in the scan range of 400–4000 cm^{-1} was used to identify the functional groups in the powders and measure the transmittance of nanocomposites. Inductively coupled plasma (ICP, Agilent 7900, Japan) tests were conducted to determine the concentration of metal ions in solution.

3. Results and discussion

Fig. 1 shows the XRD patterns of Y_2O_3–MgO nanopowders calcined at 600–1100 °C. The nanopowders are composed of amorphous phases with slight diffraction peaks associated with cubic Y_2O_3 and MgO phases at 600 °C. With an increase in the calcination temperature, the diffraction peaks gradually become more intense and narrow, indicating better crystallization of the metal oxides and an increase in their crystalline size. The calculated average sizes of the calcined Y_2O_3–MgO nanopowders, based on the peak broadening effect using the Scherrer formula [22], are summarized in Fig. 2. The crystalline size increases from 10 nm to 22 nm as the calcination temperature increases from 800 °C to 1100 °C.

The specific surface areas of Y_2O_3–MgO nanopowders calcined at 800–1100 °C are shown in Fig. 2. When calcination temperature increases from 800 °C to 1100 °C, the specific surface area decreases from 59.33 m^2/g to 29.32 m^2/g, corresponding to an increase on the particle size. TEM analysis was carried out to further verify the growth trend of particles with the calcination temperature. As shown in Fig. 3(a), the nanopowders calcined at 800 °C contain fine particles with a narrow size distribution (20–23 nm). When the calcination temperature increases to 1100 °C, the average particle size approaches 50 nm, as seen in Fig. 3(b). This is because that a higher calcination temperature leads to a larger particle size, which is consistent with the size-calculations in Fig. 2.

Fig. 4 shows the weight change of Y_2O_3–MgO nanopowders calcined at 800, 900, 1000 and 1100 °C after exposure to identical conditions of 30% relative humidity at 25 °C. There is an apparent weight-gain tendency for all the nanopowders. Moreover, the nanopowders calcined at high temperatures gain weight more slowly than those calcined at low temperatures. The nanopowders calcined at 1100 °C have the lowest final weight gain of 1.4%, while those calcined at 800 °C have the highest weight gain of 3.0% after 160 min. This suggests that the hydroscopic nature of the nanopowders gradually weakens with an increase in calcination temperatures, which is ascribed to low specific surface areas or large particle sizes.

In order to distinguish the impacts of Y_2O_3 and MgO on the moisture absorption of Y_2O_3–MgO nanopowders, the nanopowders calcined at 800 °C with different molar ratios of MgO/Y_2O_3 were exposed to identical condition of 30% relative humidity at 25 °C to test the weight change, too. Fig. 5 shows that the weight of these nanopowders tend to increase with time and the nanopowders with higher molar ratios of MgO/Y_2O_3 have faster weight gains, demonstrating that it is easier for MgO to absorb moisture from the ambient atmosphere. In addition, theY_2O_3–MgO nanopowders calcined at 800 °C were characterized by FT-IR spectroscopy, along with the Y_2O_3 and MgO nanopowders which were synthesized and calcined under the same conditions. As shown in Fig. 6, the absorption bands in the 2500–3700 cm^{-1} (4–2.7 μm) region are assigned to the stretching vibration of O–H [12] and the tied absorption peaks at around 1430 cm^{-1} (7 μm) are attributed to the vibration of carbonate groups [16]. O–H forms by the reaction between absorbed moisture and oxides, and it tends to absorb carbon dioxide to form carbonate groups. The intensity of absorption bands in the 2500–3700 cm^{-1} region and tied absorption peaks at around 1430 cm^{-1} is stronger in the spectra of MgO and Y_2O_3–MgO nanopowders than in the spectrum of Y_2O_3 nanopowders. In addition, the absorption peaks at 1620 cm^{-1}, attributed to bending vibration of H–O–H [12] due to the absorbed moisture, are only visible in the spectra of MgO and Y_2O_3–MgO nanopowders. These results indicate that Y_2O_3–MgO nanopowders exhibit strong moisture absorption and the presence of MgO helps the

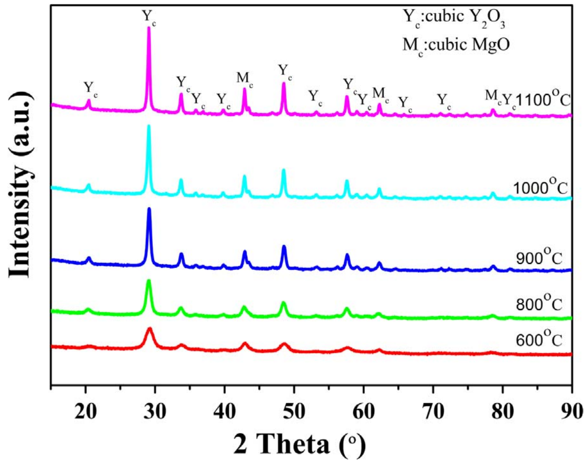

Fig. 1. XRD patterns of Y_2O_3–MgO nanopowders calcined at different temperatures.